Intuitive, Online, Simultaneous, and Proportional Myoelectric Control Over Two Degrees-of-Freedom in Upper Limb Amputees

Ning Jiang, *Member, IEEE*, Hubertus Rehbaum, *Student Member, IEEE*, Ivan Vujaklija, Bernhard Graimann, and Dario Farina, *Senior Member, IEEE*

***Abstract*—We propose an approach for online simultaneous and proportional myoelectric control of two degrees-of-freedom (DoF) of the wrist, using surface electromyographic signals. The method is based on the nonnegative matrix factorization (NMF) of the wrist muscle activation to extract low-dimensional control signals translated by the user into kinematic variables. This procedure does not need a training set of signals for which the kinematics is known (labeled dataset) and is thus unsupervised (although it requires an initial calibration without labeled signals). The estimated control signals using NMF are used to directly control two DoFs of wrist. The method was tested on seven subjects with upper limb deficiency and on seven able-bodied subjects. The subjects performed online control of a virtual object with two DoFs to achieve goal-oriented tasks. The performance of the two subject groups, measured as the task completion rate, task completion time, and execution efficiency, was not statistically different. The approach was compared, and demonstrated to be superior to the online control by the industrial state-of-the-art approach. These results show that this new approach, which has several advantages over the previous myoelectric prosthetic control systems, has the potential of providing intuitive and dexterous control of artificial limbs for amputees.**

***Index Terms*—Muscle synergy, myoelectric signal processing, non-negative matrix factorization, prosthetic control.**

I. Introduction

THE MYOELECTRIC signal (EMG) has been used as the control source for multi-function prostheses for decades. To control different functions, in current commercial devices there is the need to carefully select independent signal sites, which requires extensive experience from the prosthetist. Further, due to the limited independent sites at the residual limb, commercial hand/wrist prostheses mostly control one degree-of-freedom (DoF) at a time, and a selection mechanism is required to switch between different DoFs (e.g., wrist to hand).

To increase the functionality of myoelectric controlled upper limb prostheses, research efforts have been focused on advanced processing of the surface EMG, so that more neural control information can be extracted. To this end, pattern recognition algorithms have been extensively investigated [1]. However, after several decades of research and development, the control scheme provided by these algorithms remains sequential (only one function can be articulated at a time) and on/off (any function can be either on or off). Although combined functions or movements can be treated as additional classes [2], this approach may require an extensive training when the number of discrete functions increases. In addition, proportional control based on pattern recognition algorithms has been implemented as a separate step after the classification step [3], usually with class-based channel coefficients (the mutex approach), as reviewed in [4].

In contrast to the sequential on/off control provided by pattern recognition, the neuromuscular system activates DoFs simultaneously and proportionally. This sharp contrast in the control paradigm is one of the main reasons that there are currently no commercial prostheses based on the pattern recognition approach [5]. As such, it would be highly desirable to achieve intuitive, simultaneous and proportional myoelectric control over multiple DoFs.

Recently, the muscle synergy concept, explored by non-negative matrix factorization (NMF) of EMG signals, has been identified as a promising approach for decoding multiple DoFs from the EMG [6]. For example, it was shown that eight muscle synergies can be extracted from 11 intra-muscular EMG signals from 11 static hand postures [7]. These synergies can be used to predict muscle activities of as many as 20 new hand postures. However, only static postures (no proportional component) were considered, and the potentiality of this approach for simultaneous control was not demonstrated.

In the present study, we propose a biologically inspired approach for estimating wrist–hand kinematics from surface EMG signals. The proposed method is based on our previous study [6] in which static forces were estimated offline in healthy subjects and extends it to the estimation of wrist kinematics, online, in amputee subjects, comparing the results with the industrial state-of-the-art of prosthetic control. The method is based on the

Manuscript received February 08, 2013; revised July 03, 2013; accepted August 02, 2013. Date of publication August 26, 2013; date of current version April 28, 2014. This work was supported by the European Commission under Grant 251555 (AMYO) and Grant 280778 (MERIDIAN), by the German Ministry for Education and Research (BMBF) via the Bernstein Focus Neurotechnology (BFNT) Göttingen, under Grant 01GQ0810, and by the European Research Council (ERC) via the ERC Advanced Grant DEMOVE (267888). N. Jiang and H. Rehbaum equally contributed to this work.

N. Jiang, H. Rehbaum, and D. Farina are with the Department of Neurorehabilitation Engineering, Bernstein Center for Computational Neuroscience, University Medical Center Göttingen, Georg-August University, 37075 Göttingen, Germany (e-mail: ning.jiang@bccn.uni-goettingen.de; hubertus.rehbaum@bccn.uni-goettingen.de; dario.farina@bccn.uni-goettingen.de).

H. Rehbaum, I. Vujaklija, and B. Graimann are with the Strategic Technology Management, OttoBock HealthCare GmbH, Duderstadt, 37115, Germany (e-mail: ivan.vujaklija@bccn.uni-goettingen.de; bernhard.graimann@ottobock.de).

Color versions of one or more of the figures in this paper are available online at http://ieeexplore.ieee.org.

Digital Object Identifier 10.1109/TNSRE.2013.2278411

TABLE I
SUMMARY OF THE CHARACTERISTICS OF THE SUBJECTS WITH LIMB DEFICIENCIES

Sub ID	Age	Amp. Time	Amp. Type	Function performed
AG1	38	congenital	Right side, transradial	Wrist fle/ext, rotation
AG2	72	30 years	Left side, transradial	Wrist fle/ext, rotation
AG3	46	3 years	Left side, transradial	Wrist fle/ext, rotation
AV1	30	2 years	Right side, transradial	Wrist fle/ext, rotation
AV2	24	congenital	Left side, transradial	Wrist fle/ext, rotation
AV3	68	32 years	Left side, transradial	Wrist fle/ext, rotation
AV4	14	1 year	Left side, transhumeral, TMR	Elbow fle/ext, hand open/close

muscle synergy model, where the low-dimensional neural command (control signals) of the wrist is transformed into the activities of muscles involved in dynamic, unconstraint wrist contractions. The high-dimensional surface EMG signals are thus factorized into a set of control signals of low dimension and a synergy matrix that models the transformation of control signals into higher-dimensional neural drive to individual muscles. The control signals are used directly by the user in an online paradigm with visual feedback representing specific prosthetic commands. Since it is based on factorization, this approach is in principle unsupervised, although we will apply it with a calibration stage. The algorithm was implemented online and used by subjects with transradial limb deficiency and able-bodied control subjects. Preliminary results of this study have been earlier reported in an abstract version [8].

II. METHODS

A. Subjects

Seven men with unilateral limb deficiencies (14–72 year old) participated in the study. Four of them had a transradial amputation, two a congenital malformation, missing the hand from the wrist. A seventh subject with transhumeral amputation participated. The characteristics of the subjects with limb deficiency are summarized in Table I. In addition, seven able-bodied subjects (three female, four male, 25–56 years old) participated in the study, as control subjects. All subjects read and signed the informed consent and the study was approved by the local ethic committees.

B. Experiment Protocol

During the experimental session, the subject seated comfortably, with both upper limbs in neutral position (residual limb pointing downwards, at the side of the body). Different from previous approaches that require sample-by-sample labeled data [6], [9]–[11], where EMG signals were recorded concurrently with the kinematics for obtaining a training set of signals, the current approach does not require a labeled dataset. As discussed in Section II-C, the intended activation at multiple DoFs of the subject was based on the estimation of a latent synergy matrix from the EMG signals, which was assumed to be constant over different contractions. The synergy matrix can be estimated by factorizing any multi-channel surface EMG signal without any kinematic reference.

1) EMG Acquisition: Because the experiments took place in two locations, the measures were performed with two different EMG electrode and acquisition systems. For all intact limb subjects, 16 monopolar electrodes (Ambu Neuroline) were placed equidistantly in pairs at the thickest part of the left forearm. This position was approximately 1/3 distal, measured from the olecranon process to the styloid process of the ulnar. The inter-electrode distance was on average 23 mm. For AG2 and AG3, the same electrode placement as for the able-bodied subjects was used on the residual limb. For AG1, only 14 monopolar electrodes were placed equidistantly in the same manner, due to a limited circumference of the residual limb. In these subjects (intact-limb, AG1, AG2, AG3), the surface EMG signals were acquired by a commercial biosignal amplifier (OT Bioelettronica EMGUSB2, Italy) at a sampling rate of 2048 Hz and using 12 bit for A/D conversion, with a 3–900 Hz band-pass and a gain of 500. For the subjects AV1-AV4, the surface EMG was acquired using a proprietary signal detection and acquisition system (Otto Bock Axon-Bus), where eight active bipolar commercial prosthetic electrodes were placed equispaced around the stump by a custom-made harness. The signals were amplified by a variable gain and sampled by the integrated A/D converter at 1000 Hz and 10 bit. The inter-electrode distance of the bipolar systems was 20 mm.

2) Calibration Phase: In this study, the user intentions, i.e., the intended activation levels at different DoFs was obtained by estimating a latent synergy matrix using the data acquired in a short calibration phase. In contrast to previous studies, where kinetic [6], [9] or kinematic labels [10], [11] were used for training an estimator, these sample-by-sample labels were not needed in the current approach. Thus, the calibration included only EMG signal recordings during free, dynamic movements of the subjects. The only restriction imposed for these movements was that each single DoF was activated at a time. For all subjects, except AV4, the selected DoFs were wrist flexion/extension (DoF1) and wrist pronation/supination (DoF2), as these two DoFs are functionally the most important for transradial amputees [12] other than intrinsic hand functions, and there are recent attempts to realize prostheses that have active control of these two DoFs [13]. For AV4 (transhumeral amputation), the two articulated DoFs were elbow flexion/extension and hand open/close, because these were the only functions available after a targeted muscle reinnervation surgery (TMR) [14] following the amputation, and are functionally most important for this user. The contractions performed in this phase were referred to as the calibration contractions and were four (with full range of motion) for each DoF. The execution of all calibration contractions required less than 3 min and no kinematic/kinetic data were recorded during the calibration phase. The acquired raw EMG signals during this phase were recorded with a customized package on MATLAB platform, and used to calibrate the non-negative matrix factorization (NMF) estimator (see Section II-C). After the estimator was calibrated, the online validation phase started.

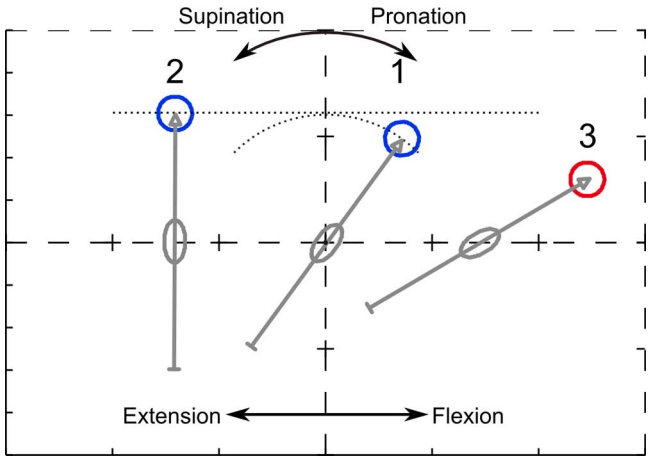

Fig. 1. Online feedback for the subjects during the validation phase. One example for each of the three types of targets is presented. Targets 1 and 2 are examples of those requiring activation of one DoF only, while target 3 requires simultaneous activations of both DoFs. The illustration shown is for left-handed subjects, and the directions of the functions are reversed for right-handed subjects.

3) Online Validation Phase: After calibration, the subject was instructed to perform an online validation test, where the subject controlled a feedback arrow on the monitor of a PC. The horizontal displacement and rotation angle of this feedback arrow were determined by the control signals, extracted online from the surface EMG with inversion of the synergy matrix (see Section II-C). It is effectively a position control approach, i.e., when there is no surface EMG activity, the arrow will return to its initial position. For all subjects, except for AV4, the left and right movement of the arrow represented wrist flexion and extension, while the clockwise and counterclockwise rotation represented wrist supination and pronation. For subject AV4, left and right movement of the arrow represented elbow flexion and extension, while clockwise and counterclockwise rotation represented hand open and close. The correction factors [see (6)] were determined at this point for each subject, so that potential directional reversal (due to the indeterminacy of NMF) could be corrected, and the full range of motion in each DoF could be reached. This process usually took less than one minute. Then, each subject was instructed to place the tip of the arrow within circular targets that appeared randomly in different places on the screen (Fig. 1).

The area of the target was 1.4% of the entire working space. If the tip was placed within a target circle for more than 300 ms within a 20 s time interval, the task was considered successfully completed. Otherwise, the attempt was considered a failure. Three groups of targets were presented within the reaching range of the subject. The targets of the first groups were located on the unit-circle with random rotation angles, so that the subject could complete the task by articulating DoF2 (pronation/supination) only, thus rotating the arrow; the targets in the second group had the same horizontal height as the arrow's length, with random left–right displacement, so that the subject could complete the task by articulating DoF1 (flexion/extension) only, thus moving the arrow to the left or right; the targets of the third group were randomly placed such that the subject had to simultaneously articulate both DoFs for at least a part of the task to successfully hit the circle. This is because in position control mode, it is not possible to hit the target by sequentially articulating the DoFs. Ten targets per group were presented to each subject. To measure the performance of these tasks, three indices were calculated: task completion rate (α), task completion time (t_c), and efficiency coefficient (Γ). The task completion rate (α) was defined as the number of completed tasks over the total number of attempted tasks. The task completion time (t_c) was the time needed by the subject to complete the successful attempts. The efficiency coefficient Γ was defined as the ratio between the length of the optimal path from the initial point to the target (the dotted lines in Fig. 2) and the length of the actual path taken by the subject (a value of 100% indicates a perfect execution), similar to the

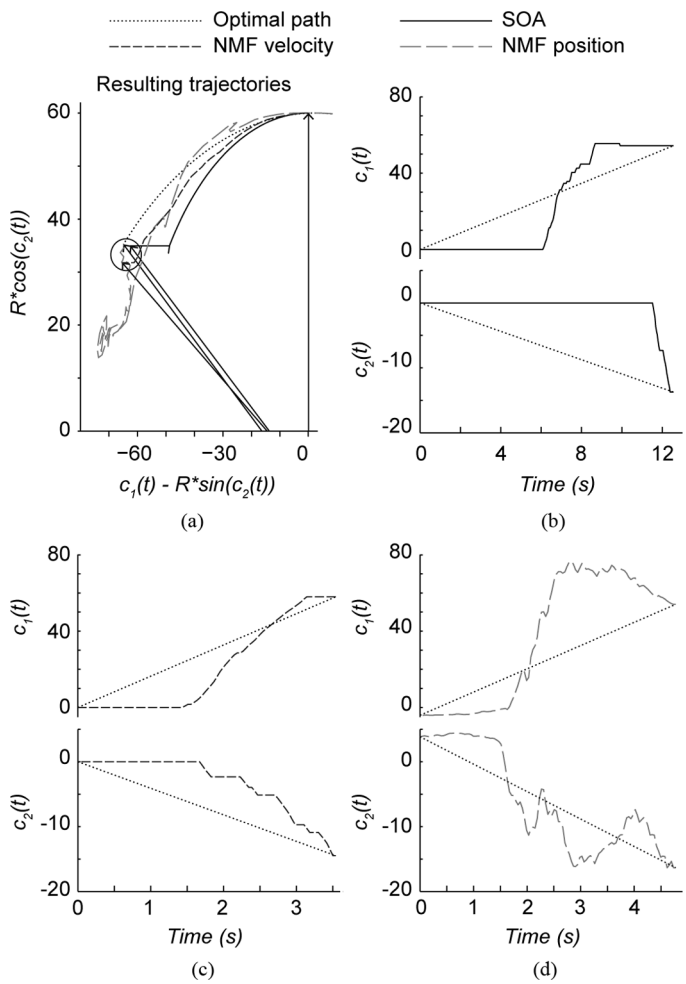

Fig. 2. Representative trajectories of the tasks in the validation phase of the experiment, with all three control approaches. The data shown are from subject AG3. (a) The trajectories shown to the subject. The task for the subject was to move the arrow (initially in vertical position) to hit the target (circle). The optimal trajectory is indicated by the dotted line, and the trajectories from the three control approaches are indicated by solid (SOA), dark dashed (NMF velocity) and light dashed (NMF position) lines, respectively. The control signals at the two DoFs, from which the trajectories in (a) are calculated, are shown in (b), (c), and (d) for the SOA, NMF velocity, and NMF position, respectively [see (4)–(6)]. The arbitrary constant R is used to represent the length of the arrow (see Fig. 1). For the data shown, the (t_c) for the three control approaches are 12.6 s, 3.54 s, and 4.77 s, respectively. The (Γ) for the three control approaches are 88.5%, 89.5%, and 44.7%, respectively. Note the long time needed for mode switch in (B), from 8.7 s to 9.9 s.

definition in [15]. However, the optimal path in the current setup was different from the shortest path defined in [15], i.e., the straight path from the starting point to the target point. This is because in the current setup, the control variables were the angles in the two DoFs and not the Cartesian coordinates, as in [15]. Due to the different instrumentations used, (Γ) was not measured for subjects AV1-AV4.

Algorithm

The basic synergy matrix estimation algorithm is based on the minimally supervised NMF algorithm, as proposed in [6]. For the sake of completeness, the algorithm is presented here briefly. The root mean square (rms) values of the N-channel surface EMG, denoted as $\boldsymbol{Z}(t)$, can be approximated by the product of a $2M$-dimensional latent control signals, namely $\boldsymbol{C}(t)$, and a synergy matrix $N \times 2M$ vector W

$$\boldsymbol{Z}(t) = W \cdot \boldsymbol{C}(t). \tag{1}$$

In the current study, the rms values were obtained by non-overlapping 100-ms processing windows. In this way, the control signals were effectively sampled every 100 ms (at 10 Hz). The two terms on the right hand side of (1) are unknown but all elements are assumed to be non-negative. With the non-negative assumption, the activation of the ith DoF can be represented by two non-negative control signals, namely c_i^p and c_i^n , for the positive and negative direction of the ith DoF, respectively. It follows that (1) becomes

$$\boldsymbol{Z}(t) = [W_1^p, W_1^n \cdots W_M^p W_M^n] \cdot \begin{bmatrix} c_1^p(t) \\ c_2^n(t) \\ \vdots \\ c_M^p(t) \\ c_M^n(t) \end{bmatrix}. \tag{2}$$

In general, there are infinite numbers of solutions to (2), which is known as the indeterminate property of NMF. It is therefore not possible to use the NMF algorithm directly to extract meaningful control signals in the context of myoelectric control. To address this problem, prior information was applied to constraint the possible solutions of (2) in a "divide and conquer" approach. This was done by a specifically designed experimental protocol, in which the subject performed motions that selectively activated single DoF during the calibration phase [see Section II-B(2)]. This constraint limited the space of possible solutions to only one (apart from the indetermination in the scale of the control signals). Considering the case that only the ith DoF is articulated (as in the calibration phase of the current study), all elements in $\boldsymbol{C}(t)$ should be zero except $c_i^p(t)$ and $c_i^n(t)$ and (2) reduces to

$$\boldsymbol{Z}_{[i]}(t) = [W_i, W_n] \cdot \begin{bmatrix} c_i^p(t) \\ c_i^n(t) \end{bmatrix} \tag{3}$$

where $\boldsymbol{Z}_{[i]}(t)$ denotes the rms of the N-channel surface EMG when only the ith DoF is articulated. In this approach, the problem of solving (1) is reduced to solving M instances of (3), where all columns of W' can be estimated in a DoF-wise fashion. The indeterminacy is therefore constrained within individual problems in (3), and is trivially resolved *a posteriori*, as presented next (Section II-D). To enhance the robustness of the online performance, the multilayer NMF procedure was used [16], where a number of NMF factorizations were concatenated. The input to the first NMF was the rms of the recorded EMG signals, and its output was the input to the second NMF, and so on. The optimal number of NMF procedures was determined by a preliminary analysis on pilot data and was set to 100 for all subsequent analyses. Extensive details of this DoF-wise NMF algorithm, specifically designed for simultaneous and proportional myoelectric control, can be found in [6].

C. Online Estimation of the Control Signals

Using the algorithm described above, the synergy matrix, W, in (1) was estimated from the calibration data. In order to estimate the control signals related to the intended activation levels of the articulated DoFs, the inverse model was applied. For this purpose, the pseudo inverse W^+ of W' was calculated using the Moore–Penrose algorithm [17] and applied to estimate the control signals

$$\mathrm{C}(t) = W^+ \cdot \boldsymbol{Z}(t) \tag{4}$$

where

$$\boldsymbol{C}(t) = \begin{bmatrix} c_1^p(t) \\ c_1^n(t) \\ \vdots \\ c_M^p(t) \\ c_M^n(t) \end{bmatrix}. \tag{5}$$

Note that each component of $\boldsymbol{C}(t)$ in (5) is normalized with respect to its respective maximum value. This component-wise normalization is to ensure that no components would be overshadowed by other components due to their differences in magnitude, so in the subsequent calculation [see (6) below], each pair $c_i^p(t)$ and $c_i^n(t)$, can be combined as the control signal of one DoF. In the current application, $\mathrm{M} = 2$ since two DoFs were involved, and since it was necessary to control each DoF independently when needed as well as simultaneously. The need of independent control is reflected in the calibration phase, based on single DoF activations. With this approach, it has been shown previously for the shoulder–elbow complex that the number of synergies is always twice the number of degrees of freedom [18]. This approach is optimal for myoelectric control since it provides signals directly associated to the DoFs and with the linear property that allows linear combination of the primitive signals for simple simultaneous control of multiple DoFs. The control signals, estimated as in (4), were further scaled by the scalar correction factors τ_{ij} to obtain the final control signals, which were then presented to the subject to control the arrow. These scalar correction factors were used to account for the indetermination of the signal power in the factorization process

$$\begin{aligned} c_1(t) &= \tau_{11} \cdot c_1^p(t) - \tau_{12} \cdot c_1^n(t) \\ c_2(t) &= \tau_{21} \cdot c_2^p(t) - \tau_{22} \cdot c_2^n(t) \end{aligned} \tag{6}$$

where the multiplicative factors τ_{ij} were determined such that the resulting control signal, i.e., $\mathbf{C}(t) = [c_1(t); c_2(t)]$, matched the range of joint angles in the respective DoFs, determined by

the subject during the calibration phase. This is a further step in resolving the indeterminate scaling problem of the NMF solution to (3), in a *post-hoc*, subject-specific basis. The control signals $\mathbf{C}(t)$, low-pass filtered at 6 Hz (kinematic bandwidth [19]), were then used by the subject, without further processing, for controlling the virtual arrow and thus for expressing activations at the articulated DoFs. Although this type of association may not be perfect, it was assumed that the subject could compensate for the differences using the online feedback. This assumption was tested and confirmed experimentally (see Sections III and IV).

D. Comparison With State-of-the-Art

From the 14 subjects tested, four representative subjects (three able-bodied subjects, and one amputee subject) participated in an additional second experiment, with the purpose of comparing the proposed control paradigm with the industrial state-of-the-art (SOA) control. Depending on their prior experiences with myoelectric control, the three able-bodied subjects were considered as an expert (H2), intermediate (H5), and naïve (H7). The amputee subject (AG3) routinely uses a commercial myoelectric prosthesis.

The industrial SOA was implemented as the standard two-control sites with the one-site-one-function method. Through visual inspection of prosthetic experts, two channels from all available channels with minimal cross-talk were selected as the control sites. The activation thresholds of the two channels were also determined by the standard procedure in prosthetic fitting, allowing easy activation of the functions and the mode-switch trigger. Once the threshold of one of the channels was exceeded, the corresponding function would be selected (e.g., wrist flexion or extension). When the two thresholds were simultaneously exceeded, a mode switch would take place, e.g., from wrist flexion/extension mode to wrist supination/pronation mode.

Thirty fixed targets, 10 for each category, were presented in random order for both the industrial SOA and the proposed paradigm. The industrial SOA was implemented in velocity control mode, so the third type of targets could be reached (in position mode these targets are not reachable with the industrial SOA). The proposed paradigm was implemented in both velocity mode and position mode (the latter is the same control as in the main experiment). The same performance measures described for the first experiment were used for comparing the SOA control and the proposed approach.

E. Statistics

ANOVA tests were conducted on t_c and (Γ) . For the main experiment on all subjects, the three factors considered were the subject type (amputee and able-body), the subjects, and task difficulty (single DoF activation and two DoFs activations). The subject was a random factor and was nested within the factor of subject type. A full ANOVA model was conducted first. In case of no significant interactions, the effects of the interactions were pooled and only the effects of the main factors were analyzed. For the comparison tests between the proposed paradigm and the industrial SOA, two-way ANOVA with repeated measures within one factor were conducted on the data from each subject. The factors were target type (three target types) and control scheme. The three types of the control scheme were industrial SOA, NMF position and NMF velocity. Whenever ANOVA detected a significant interaction, a one-way ANOVA was conducted on one of the factors by fixing the level of the other factor. When there was no significant interaction, the interaction effect was pooled and only the main effects were analyzed. Multi-comparison was conducted in case of any significance. The significance level was set at 0.05 for all tests.

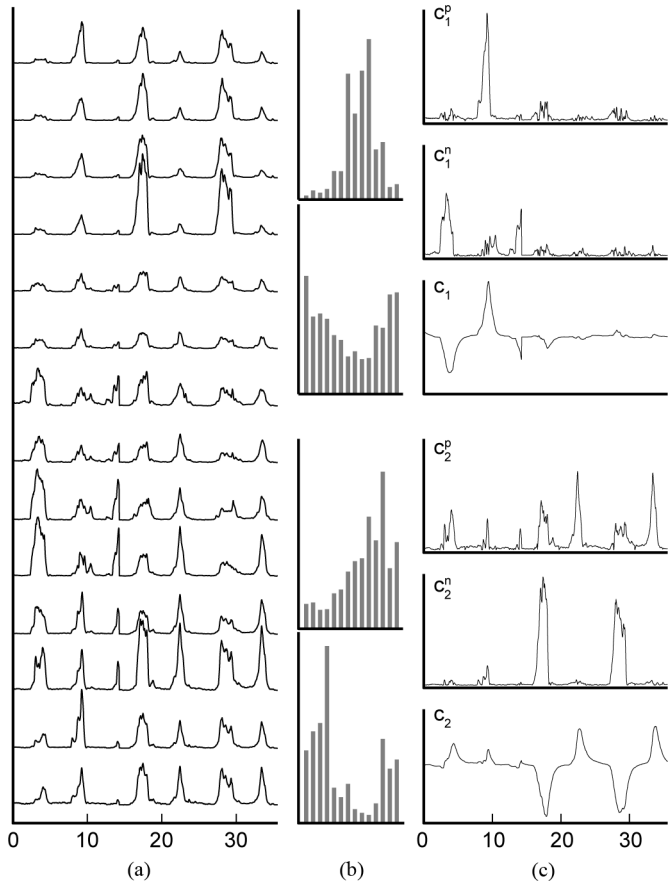

Fig. 3. Illustration of the proposed approach. Data shown are from subject AG1 (only 14 EMG channels were used). Column A are the rms values of the raw EMG signals, and column B are the four estimated synergies (the top two for DoF1 and the bottom tow for DoF2). In column C, the control signals in separate directions and final control signals are presented [see (6)].

III. Results

Representative EMG data, extracted synergies, and estimated control signals from an amputee subject are presented in Fig. 3. The trajectories of a target hitting test (a type 3 target) from one amputee subject for all three control modes are presented in Fig. 2.

A. Estimated Synergy Matrix

The four average synergies over all the able-bodied subjects are presented in Fig. 4. As shown in the figure, there is consistency in the synergy matrix obtained from different subjects, particularly the two synergies corresponding to wrist flexion (synergy 1) and extension (synergy 2), which had smaller variability across subjects (see standard deviations in the bar plots).

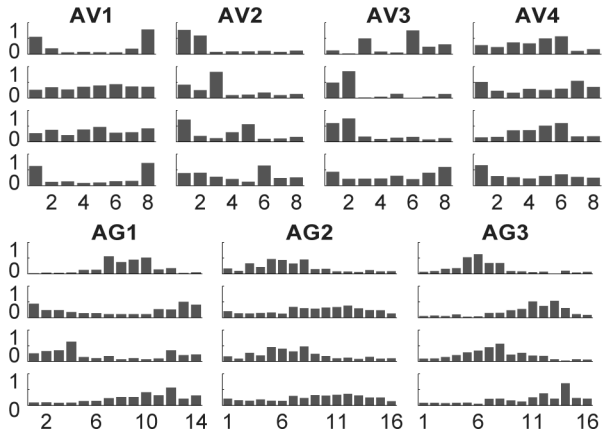

Fig. 4. Average synergy matrix from all able-bodied subjects. Each bar is the mean value across subjects of the corresponding electrode site, and the vertical bars indicate standard deviation across subjects.

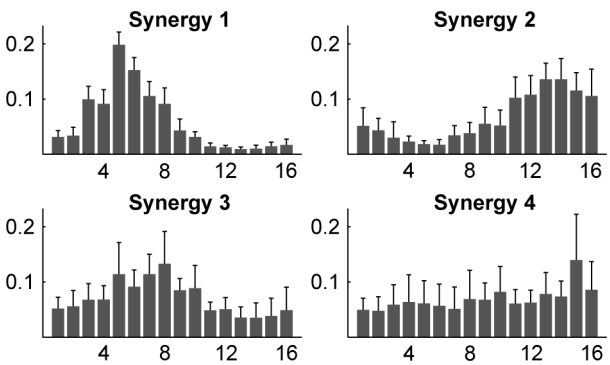

Fig. 5. Synergy matrixes of each of the seven amputee subjects. Each bar corresponds to the synergy coefficient at each electrode site.

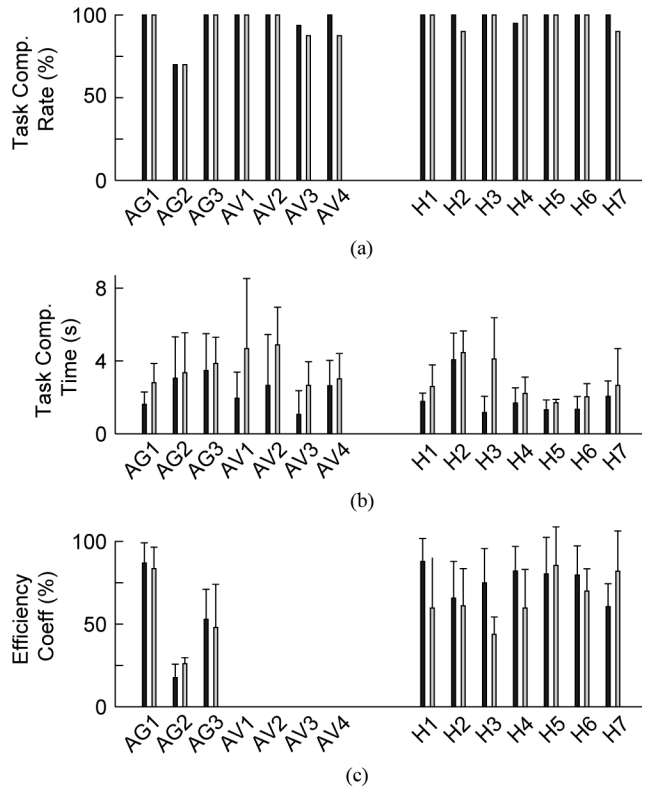

Fig. 6. Online control performance of all subjects: task completion rate α (a), task completion time t_c (b), and execution efficiency (Γ) (c). In all plots, amputee data are on the left and able-bodied subject data are on the right. Note that α and t_c are available from all seven amputee subjects, while (Γ) is only available from three amputee subjects due to different instrumentations used for AV1-AV4 (see Section II-C3). The black bars refer to single DoF tasks, and the grey bars to two-DoF tasks.

Consistency of synergies across subjects is a finding in agreement with earlier reports [10]. Such consistency confirmed the validity of the underlying physiological model on which the algorithms of the current study is based. The obtained synergy matrix of each individual amputee subject is shown in Fig. 5. It is evident in the figure that, due to the differences in the anatomy of the residual limbs across amputee subjects, the synergies extracted from the amputees were largely variable across the subjects, such that each amputee had a specific synergy matrix.

B. Online Control Performance

The descriptive statistics of the target hitting tests are summarized in Fig. 6, for amputees and able-bodied subjects. The high task completion rate ($> 90\%$ in all cases; able-bodied subjects average 95.3%, amputees average 93.5%) in both subject groups with targets of both difficulty levels indicated that all subjects were able to accomplish the online control task. On average, able-bodied control subjects seemed to perform slightly better than the amputee subjects, in all three performance measures. For both subject groups, the targets requiring simultaneous and proportional activation usually resulted in worse performance scores than those requiring activation of only one DoF (Fig. 6), indicating the different difficulties of the targets. ANOVA analyses were performed on and (Γ) . For both tests, no significant interaction among the factors was found. After the interaction effect was pooled, no statistical significance was found between amputee subjects and able-bodied subjects for both t_c and (Γ) ($p = 0.087$ and $p = 0.135$). For the factor of target type, both response variables were found to be statistically different for different target types, with the respective p-values of 0.015 and 0.002, indicating that the online performance depended on the task difficulty. Also, the factor subject was significant for both response variables ($p < 10^{-3}$ for both cases), indicating significant variability among the subjects within each group.

C. Comparison With the Industrial SOA

In the second experiment, the task completion rates were 100% for the able-bodied subjects and 94.4% for the participating amputee. The descriptive statistics are presented in Table II. In general, the more experienced the subject was with myoelectric control, the better performance was achieved, for all control schemes. As expected, the NMF control schemes were superior to the SOA control, as indicated by the consistent shorter for all subjects. As discussed above, the path efficiency coefficient gives SOA control an inherent advantage over NMF control because inadvertent activations of the non-target DoF could take place for NMF control schemes (see Fig. 2). In spite of this advantage, for the NMF velocity control scheme, the Ã values were similar to SOA values (Table II). The ANOVA analysis (see Table III) revealed further information. For all

TABLE II
DESCRIPTIVE STATISTICS FOR EXPERIMENTS FOR SOA AND NMF CONTROL COMPARISON

		SOA	NMF pos.	NMF vel.
H2	t_c	2.10±2.00	1.40±1.35	1.71±0.64
	Γ	88.97±18.67	66.87±24.36	85.70±13.14
H5	t_c	1.85±2.58	1.61±1.90	1.79±0.73
	Γ	89.61±22.74	64.01±22.74	86.96±13.66
H7	t_c	3.69±3.62	2.92±3.82	2.50±1.86
	Γ	88.02±19.96	48.76±23.30	80.91±22.30
AG3	t_c	5.67±4.91	4.51±2.88	5.00±2.97
	Γ	78.71±22.71	48.21±18.95	64.40±22.76

subjects, the consistent worse performance (longer and smaller (Γ)) of the third target type (DoF12) than the first two target types (DoF1 and DoF2) indicated that simultaneous and proportional control was more difficult than controlling the two DoFs separately. For the three control paradigms, the t_c of at least one of the NMF paradigms was significantly shorter than SOA, at least for the third target type. Specifically, for subjects H2 and AG3, both NMF paradigms had significantly shorter t_c than SOA for the third target type, while there was no significant difference for the first two target types. For H5, NMF velocity control had significantly shorter t_c than SOA for the third target type, while there was no significant difference for the first two target types. For subject H7, t_c was significantly shorter in NMF velocity control than SOA, regardless of the target type (no significant interaction of the two factors). For Ã, the two NMF paradigms produced significant worse path efficiency than SOA for subjects H2 and AG3. However, for subjects H5 and H7, no significant difference in path efficiency was found between NMF velocity and SOA. Furthermore, for AG3, NMF position control had significantly worse (Γ) than NMF velocity control. Given the inherent advantage of SOA in this measure, this is additional strong indication of the good controllability of the NMF approach.

In summary, for all subjects tested in the second experiment, at least one of the NMF control modes outperformed SOA in task completion time, particularly for the more difficult tasks (DoF12). For some subjects, there was no difference in path efficiency between NMF velocity mode and SOA control. The comparison clearly demonstrated the advantage of the proposed paradigm over the industrial SOA, due to its ability of allowing simultaneous and proportional control of the two DoFs.

IV. DISCUSSION

In this study, we demonstrated, for the first time, online, goal-directed simultaneous and proportional myoelectric control of multiple DoFs by both transradial amputees and able-bodied subjects. The myoelectric control paradigm proposed allows intuitive control for daily activity settings. The calibration part is very short, comparing with other myoelectric control setups reported in the literature, where a lengthy training phase is usually required [1]. Moreover, the calibration did not require the concomitant recording of EMG and kinematics which makes the method minimally supervised and not limited to unilateral amputees, contrary to previous approaches [9]–[11]. The contractions performed by the subject were dynamic free movements, as compared to the static isotonic and/or isometric contractions used in most studies in the literature. Further, the subjects performed contractions that only articulated single DoFs in the calibration phase, but the control algorithm was able to extrapolate automatically and allowed the subjects to control two DoFs simultaneously and proportionally in the online validation phase. Finally, the proposed strategy for extracting control signals is ideal for online adaptation since the synergy matrix can be reestimated from any set of movements.

One of the important results of this study is that no significant difference was found on all three online performance indices between the amputee and able-bodied subjects. Conversely, previous studies have shown that the performance of amputee subjects is lower than that of able-bodied subjects, for both classic pattern recognition approaches [20] as well as for simultaneous and proportional control approaches [11]. We believe that the reason for this difference is the online feedback provided to the subjects, through which the subject can actively adapt or correct the control outcome. This is evident in the trajectories shown in Fig. 2. In both NMF control approaches, the subject had overshoots and undershoots during the course of the attempt, with the one or both two angle trajectories oscillating around their optimal paths. This type of control is not possible without the online visual feedback.

Another important result of the current study is the demonstration of the good controllability of the proposed paradigm over the industrial SOA. For the targets that only require one DoF, the performance of the proposed paradigm was similar to the industrial SOA, in spite of the fact that undesired activations of the nontarget DoF was possible during the attempts for these tasks. For the tasks where activations of two DoFs were necessary, the proposed paradigm was shown to be superior. Indeed, the ability of simultaneous and proportional control is the main advantage of the proposed paradigm. During the comparison experiment, it was observed that the co-contraction based mode switch (as part of the sequential control paradigm) significantly affected the task execution. Particularly at the last stage of the target approaching, subject sometimes needed to switch several times between the DoFs, fine tuning the approaching direction. This was done much more efficiently when subject could control two DoFs simultaneously. This clear advantage makes the proposed control much more natural, which should be translated into better controllability than the industrial SOA when controlling real prostheses. The amputee subjects who participated in this study indeed expressed their preference for the proposed approach over the industrial SOA. The comparison has been done for the industrial SOA and not for the pattern recognition approach (academic SOA) since only the industrial SOA corresponds to a well-defined online paradigm. The academic SOA on the contrary has been mainly tested offline and the few cases of online implementations corresponded to very specific parameters and methods selections.

In the current study, the goal-directed task implemented was not designed to investigate the absolute task difficulty, as in [15], but rather the relative difficulty between amputee subjects

TABLE III
COMPARISON BETWEEN THE INDUSTRIAL SOA CONTROL SCHEME AND THE TWO NMF CONTROL SCHEME

SUB ID	Perf. Measures	TWO-WAY ANOVA		FOCUSED ONE-WAY ANOVA					
		Target Type	Ctrl Scheme	Target Type			Ctrl Scheme		
		Lvl. of the fixed factor →		SOA	NMF Pos.	NMF Vel.	DOF1	DOF2	DOF12
AG3	t_c	Significant Interaction		$p<$ 1(, DOF1<DOF12, DOF2<DOF12	*p=0.09*	*p=0.06*	*p=0.75*	*p=0.07*	*p=0.006,* NMFv<SOA, NMFp<SOA
	Γ	p = 0.003, DOF12<DOF1	$p<$ 1(, NMFp<SOA, NMFv<SOA, NMFp<NMFv	N/A					
H2	t_c	Significant Interaction		$p<$ 1(, DOF1<DOF12, DOF2<DOF12	p=0.020, DOF2<DOF12	p=0.33	p=0.93	p=0.12	$p<$ 1(, NMFv<SOA, NMFp<SOA
	Γ	p = 0.003, DOF12<DOF1, DOF12<DOF2	$p<$ 1(, NMFp<SOA, NMFv<SOA	N/A					
H5	t_c	Significant Interaction		$p<$ 1(, DOF1<DOF12, DOF2<DOF12	p=0.010, DOF2<DOF12	p=0.002, DOF1<DOF12, DOF2<DOF12	p=0.46	p=0.49	p=0.010, NMFv<SOA
	Γ	$p<$ 1(, DOF12<DOF1, DOF12<DOF2	$p<$ 1(, NMFp<SOA, NMFp<NMFv	N/A					
H7	t_c	p=0.008, DOF2<DOF12	p=0.03, NMFv<SOA	N/A					
	Γ	p=0.74	$p<$ 1(, NMFp<SOA	N/A					

and able-bodied control subject, and between the proposed control and the SOA industrial control. This purpose was served when the task parameters, such as circle size, dwelling time, task failure time, and maximum speed of the arrow (in the velocity mode) were consistent across subjects and control algorithms.

The proposed EMG processing algorithm is developed from the muscle synergy model. Some prior studies by other research groups also utilized the muscle synergy model under the context of myoelectric control [7], [21]. As discussed in the Introduction section, [7] was an offline analysis study on intra-muscular EMG, focusing on static hand postures, and no direct attempt was made to translate the proposed method into myoelectric control applications. The study in [21] also exploited the muscle synergy concept for myoelectric control, with a supervised linear regression approach with non-negative constraint. Further, no amputee was involved in [7], [21]. Comparing with these two prior studies, the current study explicitly exploited the concept of muscle synergy, with dedicated online experimental protocol for the application of myoelectric control. Seven amputees participated in the experiment, which is the largest number of amputee subjects in any studies on advanced myoelectric control algorithms.

The current study is based on algorithms extended from a previous offline study on able-bodied subjects performing isometric contractions for which forces were estimated [6]. However, the conditions of this prior study were substantially different from the current study that presents the online control of kinematics in dynamic tasks of both able-bodied and amputee subjects. Moreover, in [6] the calibrating time was much longer than in the present study. Another previously proposed approach for simultaneous and proportional myoelectric control is based on artificial neural networks [9], [10], where the algorithms were supervised, and labeling (kinematics data) was necessary, and only applicable for unilateral amputees (only offline results were presented in this case in [9], [10]). The proposed approach in the current study requires minimal calibration data without labeling, and is more suitable for the development of self-adaptive algorithms.

Although the algorithm design is inspired by the muscle synergy model [22], [23], it is important to underline that we do not intend to necessarily associate physiological relevance to the synergies extracted in this study. Indeed, the way in which these synergies were extracted imposed the association of two synergies for each DoF since the DoFs were independently activated. A similar result is obtained when independently activating the DoFs of the elbow and shoulder [18]. These results, however, do not imply that natural tasks involve mainly combinations of DoFs for which the number of synergies corresponds to that of DoFs (see also [18]). Despite this possible limitation, in this study the concept of synergistic activation has been successfully used to describe combinations of DoFs as the linear combination of motor modules (synergies) which allows building control signals for simultaneous and proportional control out of a limited set of signals recorded during the independent activation of separate DoFs.

The focus of this study was on the wrist flexion/extension and pronation/supination, as these are the most desired functions by the transradial amputees, other than the intrinsic hand functions [12], which are already provided by commercial prostheses. The next natural step is to include hand open/close. A previous offline study using the same signal processing approach on able-bodied subjects demonstrated the possibility of including wrist flexion/extension, pronation/supination, hand open/close, and radial/ulnar deviation [10]. This implies that in principle it is

possible to include the hand open/close function into the synergistic paradigm proposed here. However, the number of DoFs that can be controlled by amputees with this approach remains to be verified. Another important extension of the current algorithm is the inclusion of self-adaptation to enhance the robustness of the algorithm in real world scenarios by automatically recalibrating the synergy matrix over time.

In summary, we proposed a minimally supervised, online, simultaneous and proportional myoelectric control approach based on multi-channel surface EMG. With seven amputees and seven able-bodied controls, we demonstrated that both amputee subjects and able-bodied subjects were able to successfully perform real time control of virtual targets that required simultaneous and proportional activation of two important wrist DoFs: flexion/extension and pronation/supination. The performance of the two subject groups was not statistically different, with an average task completion rate of $\sim 95\%$. This study is an important step forward in the direction of the development of clinically viable multi-function upper limb prosthesis.

REFERENCES

[1] E. Scheme and K. Englehart, "Electromyogram pattern recognition for control of powered upper-limb prostheses: State of the art and challenges for clinical use," *J. Rehabil. Res. Develop.*, vol. 48, no. 6, p. 643, 2011.

[2] A. Young, L. Smith, E. Rouse, and L. Hargrove, "Classification of simultaneous movements using surface EMG pattern recognition," *IEEE Trans. Biomed. Eng.*, vol. 60, no. 5, pp. 1250–1258, Dec. 2013.

[3] B. Hudgins, P. Parker, and R. N. Scott, "A new strategy for multifunction myoelectric control," *IEEE Trans. Biomed. Eng*, vol. 40, no. 1, pp. 82–94, Jan. 1993.

[4] A. Fougner, O. Stavdahl, P. J. Kyberd, Y. G. Losier, and P. A. Parker, "Control of upper limb prostheses: Terminology and proportional myoelectric control—A review," *IEEE Trans. Neural Syst. Rehabil. Eng*, vol. 20, no. 5, pp. 663–677, Sep. 2012.

[5] N. Jiang, S. Dosen, K.-R. Muller, and D. Farina, "Myoelectric control of artificial limbs-is there a need to change focus? (In the Spotlight)," *IEEE Signal Process. Mag.*, vol. 29, no. 5, pp. 150–152, Sep. 2012.

[6] N. Jiang, K. B. Englehart, and P. A. Parker, "Extracting simultaneous and proportional neural control information for multiple-DOF prostheses from the surface electromyographic signal," *IEEE Trans. Biomed. Eng.*, vol. 56, no. 4, pp. 1070–1080, Apr. 2009.

[7] A. B. Ajiboye and R. F. Weir, "Muscle synergies as a predictive framework for the EMG patterns of new hand postures," *J. Neural Eng.*, vol. 6, no. 3, pp. 036004–036004, Jun. 2009.

[8] H. Rehbaum, N. Jiang, L. Paredes, S. Amsuess, B. Graimann, and D. Farina, "Real time simultaneous and proportional control of multiple degrees of freedom from surface EMG: Preliminary results on subjects with limb deficiency," in *Proc. 2012 Annu. Int. Conf. IEEE Eng. Med. Biol. Soc.*, Aug. 2012, vol. 2012, pp. 1346–1349.

[9] J. L. G. Nielsen, S. Holmgaard, N. Jiang, K. B. Englehart, D. Farina, and P. A. Parker, "Simultaneous and proportional force estimation for multifunction myoelectric prostheses using mirrored bilateral training," *IEEE Trans. Biomed. Eng.*, vol. 58, no. 3, pp. 681–688, Mar. 2011.

[10] S. Muceli and D. Farina, "Simultaneous and proportional estimation of hand kinematics from EMG during mirrored movements at multiple degrees-of-freedom," *IEEE Trans. Neural Syst. Rehabil. Eng.*, vol. 20, no. 3, pp. 371–378, May 2012.

[11] N. Jiang, J. L. Vest-Nielsen, S. Muceli, and D. Farina, "EMG-based simultaneous and proportional estimation of wrist/hand dynamics in uni-Lateral trans-radial amputees," *J. Neuroeng. Rehabil.*, vol. 9, no. 1, p. 42, Jun. 2012.

[12] D. Atkins, D. Heard, and W. Donovan, "Epidemiologic overview of individuals with upper-limb loss and their reported research priorities," *J. Prosthetics Orthotics*, vol. 8, no. 1, pp. 2–11, 1996.

[13] P. J. Kyberd, E. D. Lemaire, E. Scheme, C. MacPhail, L. Goudreau, G. Bush, and M. Brookeshaw, "Two-degree-of-freedom powered prosthetic wrist," *J. Rehabil. Res. Develop.*, vol. 48, p. 609, 2011.

[14] T. A. Kuiken, L. A. Miller, R. D. Lipschutz, B. A. Lock, K. Stubblefield, P. D. Marasco, P. Zhou, and G. A. Dumanian, "Targeted reinnervation for enhanced prosthetic arm function in a woman with a proximal amputation: A case study," *Lancet*, vol. 369, no. 9559, pp. 371–380, Feb. 2007.

[15] M. R. Williams and R. F. Kirsch, "Evaluation of head orientation and neck muscle EMG signals as command inputs to a human-computer interface for individuals with high tetraplegia," *IEEE Trans. Neural Syst. Rehabil. Eng.*, vol. 16, no. 5, pp. 485–496, Oct. 2008.

[16] A. Cichocki, S. Amari, R. Zdunek, R. Kompass, G. Hori, and Z. He, "Extended smart algorithms for non-negative matrix factorization," *Artif. Intell. Soft Comput.*, vol. 4029, pp. 548–562, 2006.

[17] E. H. Moore, "On the reciprocal of the general algebraic matrix," *Bull. Am. Math. Soc*, vol. 26, no. 9, pp. 394–395, Jun. 1920.

[18] S. Muceli, A. T. Boye, A. d'Avella, and D. Farina, "Identifying representative synergy matrices for describing muscular activation patterns during multidirectional reaching in the horizontal plane," *J. Neurophysiol.*, vol. 103, no. 3, pp. 1532–1542, Mar. 2010.

[19] D. A. Winter, *Movement, Biomechanics and Motor Control of Human*. New York: Wiley-Interscience, 1990.

[20] A. B. Ajiboye and R. F. Weir, "A heuristic fuzzy logic approach to EMG pattern recognition for multifunctional prosthesis control," *IEEE Trans. Neural Syst. Rehabil. Eng.*, vol. 13, no. 3, pp. 280–291, Sep. 2005.

[21] C. Choi and J. Kim, "Synergy matrices to estimate fluid wrist movements by surface electromyography," *Med. Eng. Phys.*, vol. 33, no. 8, pp. 916–23, Oct. 2011.

[22] E. Bizzi, F. Mussa-Ivaldi, and S. Giszter, "Computations underlying the execution of movement: A biological perspective," *Science*, vol. 253, no. 5017, pp. 287–291, Jul. 1991.

[23] A. d'Avella, A. Portone, L. Fernandez, and F. Lacquaniti, "Control of fast-reaching movements by muscle synergy combinations," *J. Neurosci.*, vol. 26, no. 30, pp. 7791–7810, Jul. 2006.

Ning Jiang (S'02–M'09) received the B.S. degree in electrical engineering from Xi'an Jiaotong University, Xi'an, China, in 1998, and the M.Sc. and Ph.D. degrees in engineering from the University of New Brunswick, Fredericton, NB, Canada, in 2004 and 2009, respectively.

He was a Marie Curie Fellow at the Strategic Technology Management, Otto Bock Healthcare GmbH, Germany from 2010 to 2012, and is currently a Research Scientist with Department of Neurorehabilitation Engineering, University Medical Center Göttingen, Georg-August University, Göttingen, Germany. His research interests include signal processing of electromyography, advanced prosthetic control, neuromuscular modeling, and BCI for neurorehabilitation.

Hubertus Rehbaum (S'12) received the Dipl.-Ing. degree in electrical engineering and information technology from the RWTH Aachen University, Aachen, Germany, in 2011. He is currently a Marie Curie Fellow and a Ph.D. degree candidate at the Department of NeuroRehabilitation Engineering, University Medical Center, University of Göttingen, Göttingen, Germany.

His research interests include signal processing of electromyography, advanced prosthetic control, and adaptive control algorithms.

Ivan Vujaklija received the Dipl.-Ing. degree in electrical engineering and computer science from the University of Belgrade, Belgrade, Serbia, in 2011. He is currently working toward the M.Sc. degree in biomedical engineering at the University of Lübeck, Lübeck, Germany. He is conducting an internship at the Strategic Technology Management department, Otto Bock Healthcare GmbH, Duderstadt, Germany.

His research interests include bio-signal processing, prosthetic control, and advance control algorithms.

Bernhard Graimann received the Ph.D. degree in computer science and biomedical engineering from the Graz University of Technology, Graz, Austria, in 2002.

He was a Postdoctoral Researcher at the Laboratory of Brain–Computer Interfaces, Graz University of Technology (TU Graz), Graz, Austria, and at the Institute of Automation, University of Bremen, Bremen, Germany. Since 2006, he has been a Lecturer at the Institute of Knowledge Discovery, TU Graz. In 2008, he became the Scientific Coordinator for Neurotechnology at Otto Bock HealthCare GmbH, Duderstadt, Germany. His main research interests include direct man–machine interfaces based on biosignals, biomedical signal processing, and neurorehabilitation.

Dario Farina (M'01–SM'09) received the M.Sc. degree in electronics engineering from Politecnico di Torino, Torino, Italy, in 1998, and the Ph.D. degrees in automatic control and computer science and in electronics and communications engineering from the Ecole Centrale de Nantes, Nantes, France, and Politecnico di Torino, respectively, in 2002.

During 2002–2004, he was a Research Assistant Professor at Politecnico di Torino and in 2004–2008, and Associate Professor in Biomedical Engineering at Aalborg University, Aalborg, Denmark. From 2008 to 2010, he was Full Professor in Motor Control and Biomedical Signal Processing and Head of the Research Group on Neural Engineering and Neurophysiology of Movement at Aalborg University. In 2010, he was appointed Full Professor and Founding Chair of the Department of Neurorehabilitation Engineering, University Medical Center Göttingen, Georg-August University, Germany, within the Bernstein Center for Computational Neuroscience. He is also the Chair for Neuroinformatics of the Bernstein Focus Neurotechnology Göttingen. His research focuses on biomedical signal processing, modeling, neurorehabilitation technology, and neural control of movement. Within these areas, he has (co)-authored more than 260 papers in peer-reviewed journals and over 300 among conference papers/abstracts, book chapters, and encyclopedia contributions.

Dr. Farina has been the Vice-President of the International Society of Electrophysiology and Kinesiology (ISEK) from 2010 to 2012 and is currently the President of ISEK. He is the recipient of the 2010 IEEE Engineering in Medicine and Biology Society Early Career Achievement Award for his contributions to biomedical signal processing and to electrophysiology. He is an Associate Editor of IEEE TRANSACTIONS ON BIOMEDICAL ENGINEERING.